Clays and Clay Minerals, Vol. 40, No. 1, 92–102, 1992.

FTIR STUDY OF DEUTERATED MONTMORILLONITES: STRUCTURAL FEATURES RELEVANT TO PILLARED CLAY STABILITY

KRISHNA BUKKA AND J. D. MILLER

Department of Metallurgy and Metallurgical Engineering
University of Utah, Salt Lake City, Utah 84112-1183

JOSEPH SHABTAI[1]

Department of Fuels Engineering, University of Utah
Salt Lake City, Utah 84112-1183

Abstract—FTIR studies of six partially-deuterated montmorillonites (MS) reveal the presence of two O–D stretching bands, one between 2702–2728 cm^{-1} and another near 2680 cm^{-1}. For homoionic (Li, Na, Mg, Ca, or La) Wyoming-type MS, the position of the higher frequency band, designated as $(O–D)_h$, is between 2714–2728 cm^{-1}, whereas for homoionic Cheto-type MS it is between 2702–2706 cm^{-1}. The lower frequency band, designated as $(O–D)_l$, is in the narrow range of 2674–2684 cm^{-1}. Resolution of two corresponding O–H bands, appearing near 3670 and 3635 cm^{-1}, was observed only after partial dehydroxylation of the smectites. The changes in the relative intensities of the two O–D stretching bands as a function of the smectite type and of the Lewis acidity (charge density) of the exchangeable ion were determined. For Wyoming-type MS, the intensity of the $(O–D)_h$ band is much lower than that of the $(O–D)_l$ band, whereas for Cheto-type MS, the intensity of the $(O–D)_h$ band is about equal or slightly higher than that of the $(O–D)_l$ band. The observed resolution can be ascribed tentatively to the presence of (at least) two types of octahedral OH groups in the smectites, the $(O–D)_h$ band being assigned to AlMgOH and the $(O–D)_l$ band to AlAlOH groups. Pillaring of Cheto-type MS with hydroxy-Al_{13} oligocations resulted in products showing much higher thermal stability between 400–600°C compared to that of identically pillared Wyoming-type MS. Compositional and other factors, e.g., CEC values and mode of pillaring, may cause this difference in stability.

Key Words—Deuterated montmorillonites, FITR, Pillared smectites, Thermal stability.

INTRODUCTION

Some structural features of montmorillonites, relevant to their reactivity, have not been sufficiently clarified. The most popular idealized structure for montmorillonite (Hofmann *et al.,* 1933; Magdefrau and Hofmann, 1937), shown in Figure 1, is similar in certain respects to that of pyrophyllite, as elucidated by Gruner (1934). Some incompatibility of this structural model with the observed properties of montmorillonites has been discussed by Edelman and Favejee (1940), and subsequently by Deuel *et al.* (1950). One of the objections to Hofmann's model was the absence of a quantitatively adequate provision in the structure to explain the linear swelling behavior and the high ion exchange capacity of montmorillonites. Since swelling distinguishes montmorillonites from pyrophyllites, it was reasonable to assume that the (001) surfaces in the former are somewhat different. Consequently, Edelman and Favejee (1940) proposed an alternative model structure for montmorillonites, shown in Figure 2. In this structure, some hydroxyl groups were assumed to be present at the layer surfaces, i.e., a part of the apical oxygens at the tetrahedral silicate layers were replaced with hydroxyl groups. It was also suggested that the surface hydroxyl groups participate in the swelling mechanism. There were relatively few references (McConnell, 1950; Jonas, 1955) in the older literature indicating any level of corroboration for the Edelman-Favejee structure, although some recent work on clay pillaring has tended to provide some reference to it (Plee *et al.,* 1985; Pinnavaia *et al.,* 1985; Sterte and Shabtai, 1987). Specifically, these authors assumed interaction between inverted tetrahedra at the internal silica surface and OH groups in the pillaring oligocation.

Grim and Kulbicki (1961) studied the phase transformations of montmorillonites between 600–1400°C, using continuous X-ray diffraction measurement through this temperature range. Results obtained showed that various montmorillonite samples did not yield the same crystalline phases upon heating. Consequently, such samples were divided by these authors into two broad groups termed Wyoming- and Cheto-type montmorillonites, the names referring to the locations of the samples. A significant difference observed between these two groups was that Cheto-type montmorillonites on heating went through β-quartz (900–1100°C), β-cristobalite (1150–1400°C), and cor-

[1] To whom correspondence should be addressed.

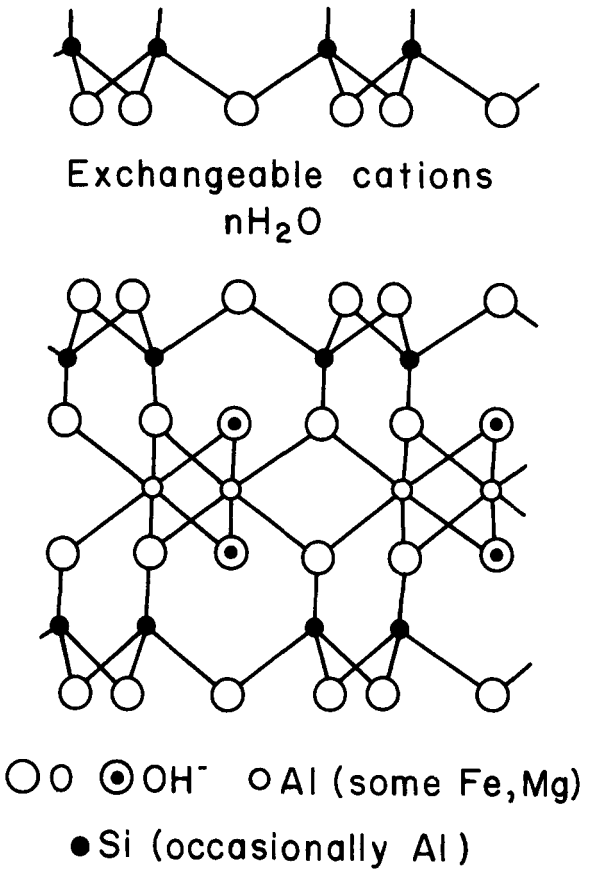

Figure 1. Structural model of montmorillonite according to Hofmann *et al.* (1933).

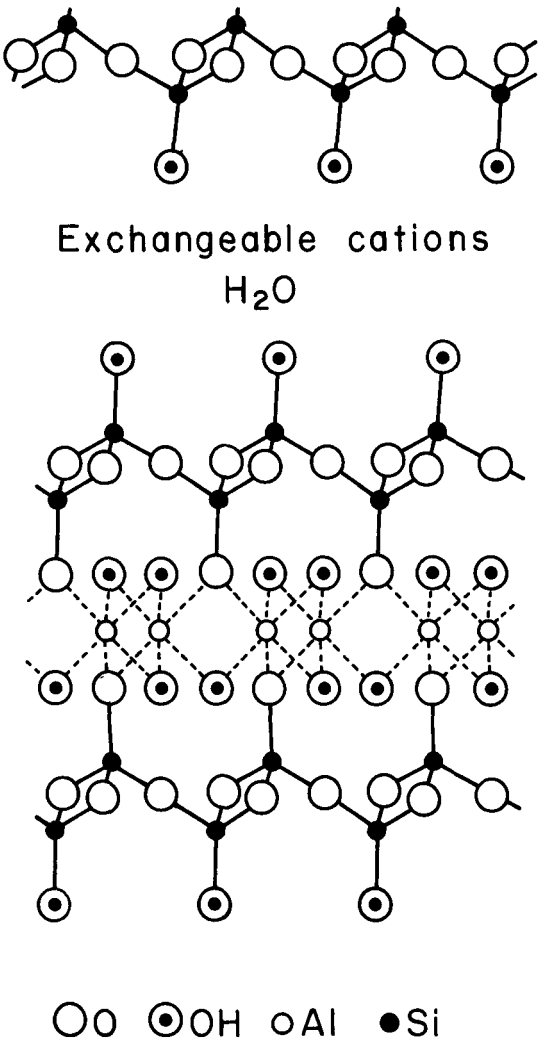

Figure 2. Structural model of montmorillonite according to Edelman and Favejee (1940).

dierite (1200–1400°C) phases without passing through a mullite phase, whereas montmorillonites of the Wyoming type went through β-cristobalite (1150–1400°C) and mullite (1400–1500°C) phases without crossing β-quartz and cordierite phases. These observations provided an indication that there could be some structural differences between the two types of montmorillonites, which become apparent only at elevated temperatures (600–1500°C). However, no attempt was made by Grim and Kulbicki (1961) to explain the differences in terms of structural variations, other than making a passing reference to the Edelman-Favejee structure. The differentiation between the Wyoming- and Cheto-type montmorillonites was further accentuated by other properties such as optical refraction (Landgraf, 1979a), dilatometrical properties (Schomburg, 1976), and X-ray diffraction intensities of glycol complexes (Landgraf, 1979b). However, specific structural differences between the above two types were considered to be slight (Solomon and Hawthorne, 1983). Some attempts were made to explain the observed differences by considering various factors, e.g., the extent of Mg^{2+} substitution in the octahedral layer, the cation exchange capacity (Landgraf, 1979a), or the crystallinity (Güven, 1979) of the two montmorillonite types.

Among recently-developed structural differentiation techniques, ^{27}Al and ^{29}Si MAS-NMR is probably one of the most powerful and promising. The usefulness of this technique has been demonstrated in structural studies of clays and related materials (Lippmaa *et al.*, 1980; Muller *et al.*, 1981; Sanz and Serratosa, 1984; Goodman and Stucki, 1984; Tennakoon *et al.*, 1986; Komarneni *et al.*, 1986; Matsumoto *et al.*, 1986; Weiss *et al.*, 1987), and of pillared clays (Plee *et al.*, 1985; Pinnavaia *et al.*, 1985; Fripiat, 1988).

Recently, Michaelian *et al.* (1987) subjected kaolinite to partial deuteration and subsequent FTIR spectroscopic analysis, and tentatively assigned an absorption band of this clay (at 3684 cm^{-1}) to an uncoupled inner surface hydroxyl group between the tetrahedral and octahedral layers. Some earlier deuteration work

https://doi.org/10.1346/CCMN.1992.0400110 Published online by Cambridge University Press

Table 1. Source, type, and cation exchange capacity of starting smectite samples.

Designation	Source (location)	Type[1]	CEC (meq/100 g)[2]
S-WY[3]	Crook County, Wyoming	Wyoming	92
S-SD[4]	Belle Fourche, South Dakota	Wyoming	79
S-CA[4]	Otay, San Diego County, California	Cheto	135
S-AZ[5]	Cheto, Apache County, Arizona	Cheto	137
S-ITOI[4,6,8]	Itoigawa, Japan	Cheto	115
S-ROKK[4,7,8]	Rokkaku, Yamagata, Japan	Uncertain[9]	116

[1] Type classification based on Grim and Kulbicki (1961).
[2] CEC values were determined by a standard USDA method, involving sequential ion exchange with sodium acetate and ammonium acetate solutions.
[3] In the Na-form.
[4] Predominantly in the NaCa-form.
[5] In the Ca-form.
[6] This sample is commercially available from Nippon Kasseihakudo Co. Ltd., Japan.
[7] Also known as Aterazawa bentonite.
[8] These samples obtained through the courtesy of Professor S. Shimoda, Institute of Geoscience, University of Tsukuba, Japan.
[9] Tentative classification as Wyoming type.

on montmorillonites (Faucher and Thomas, 1955; Roy and Roy, 1957) was carried out mainly to try and understand the nature of adsorbed water in the clay and its interactions with structural hydroxyl groups.

The present paper is concerned with an attempt to elucidate possible structural differences between Wyoming- and Cheto-type montmorillonites, and those of corresponding pillared products. For this purpose, montmorillonite samples representative of these two types were subjected to partial deuteration and the products obtained were compared by FTIR. The effect of the exchangeable cation (Li^+, Na^+, Mg^{2+}, Ca^{2+}, or La^{3+}) upon the FTIR spectral characteristics of the deuterated montmorillonite samples was also investigated. Further, representative Wyoming- and Cheto-type montmorillonites were subjected to pillaring with hydroxy-Al_{13} oligocations. The thermal stability of the pillared products obtained was compared in the temperature range of 300–600°C for the purpose of examining possible differences in pillaring behavior and obtaining information on potentially ultrastable, pillared smectites as framework materials for catalyst systems.

EXPERIMENTAL

Materials

Six smectite samples from different locations were used in this study. The designation, source, type, and cation exchange capacities of these samples are summarized in Table 1. The indicated type of the smectites is based on the classification of Grim and Kulbicki (1961). The elemental compositions of the samples, in their Na-form, are summarized in Table 2.

Three of the clay samples, i.e., S-WY, S-CA, and S-AZ, were supplied by the Source Clay Repository of The Clay Minerals Society, while the S-SD sample was obtained from American Colloid Company. The two Japanese clays studied were from Itoigawa and Rokkaku, and it was previously indicated (Grim and Kulbicki, 1961) that the former is of the Cheto type while the latter is possibly a Wyoming-type montmorillonite. The Itoigawa clay was obtained from the Suzawa, Nishiyama mines. The Rokkaku-type montmorillonite, also called Aterazawa bentonite, was obtained from the Tsukinuno mine, Nishi-Murayama, Yamagata, Japan. Some data for an apparently similar clay have been previously reported (Hayashi, 1963).

The clays included in Table 1 contained small amounts of impurities such as quartz. These impurities were removed by size fractionation, using conventional sedimentation techniques. The <2-μm fraction obtained by sedimentation of 1%-clay suspensions was free of such impurities, as determined by XRD. Elemental analyses were obtained by inductively-coupled plasma spectrometry (ICPS). SiO_2 was separately determined by the Mo blue colorimetric method.

Preparation of homoionic clays

The clays listed in Table 1 were converted by ion exchange to five different homoionic forms, viz., Li^+-, Na^+-, Mg^{2+}-, Ca^{2+}-, and La^{3+}- forms. Each of these clays was first converted to either the Na^+- or Li^+-form and subsequently to the other forms. The preparation of the homoionic forms was carried out by subjecting the purified clays to repetitive ion exchange (4 times) with aqueous (1.0 N) chloride salt solutions containing the above cations. In each case the total concentration of the chloride salt solution corresponded to five times the cation exchange capacity of the clay used. Each of the repetitive exchange reactions was carried out for a period of at least six hours with constant stirring at room temperature, except for the La^{3+}-form, which was prepared at 90°C. The exchanged clays were washed with deionized water until chloride free, and then freeze-dried.

Deuterium exchange reaction

Partial deuterium exchange was carried out by refluxing (temperature, ~98°C) a 2.5% suspension of the clay in D_2O (concentration, 99.9%; supplied by Cambridge Isotopes Ltd.) with constant stirring for 16–62 hours, using a 100 cm^3 round-bottom flask fitted with a condenser and a drying device to prevent contact with outside moisture. At the end of the reaction, the D-exchanged clay suspension was quickly cooled down, centrifuged, freeze-dried, and immediately used in the FTIR studies, taking care to avoid contact with air/moisture by the use of dry N_2 as a controlling atmosphere.

https://doi.org/10.1346/CCMN.1992.0400110 Published online by Cambridge University Press

Table 2. Elemental composition of homoionic Na-smectite samples.[1]

	Weight %[2,3]					
	S-WY	S-SD[4]	S-CA	S-AZ	S-ITOI	S-ROKK
Na_2O	0.85	1.95	4.11	3.95	3.35	3.39
K_2O	0.11	0.36	0.05	0.05	0.24	0.08
CaO	1.23	1.21	0.02	0.10	0.07	0.05
MgO	2.72	3.04	7.38	6.67	5.08	3.58
BaO	<0.01	<0.01	0.02	0.01	<0.01	<0.01
Al_2O_3	18.54	22.56	16.48	17.68	15.14	18.02
Fe_2O_3	4.06	4.16	1.15	1.55	1.05	2.34
SiO_2	62.70	61.19	59.71	58.92	68.01	64.01
TiO_2	0.10	n.d.[5]	0.18	0.24	0.23	0.20
MnO_2	0.01	n.d.[5]	0.10	0.05	0.01	0.01
P_2O_5	0.03	n.d.[5]	0.01	0.02	0.02	0.02
Total[6]	90.26	94.47	89.21	89.24	93.20	91.70

[1] Designations as shown in Table 1.
[2] Determination using samples dried at 110°C overnight.
[3] The sum of all other elements amounted to <1.1 wt. %.
[4] From Sterte and Shabtai (1987).
[5] n.d.—not determined.
[6] Totals do not include chemically-bonded water.

FTIR spectral analysis

FTIR spectra were measured with a Digilab FTS-40 IR spectrophotometer equipped with a liquid nitrogen-cooled MCT detector and a Model 3240 data system. The freeze-dried clay sample, 7–10 mg, was added to 300 mg spectrograde KBr, and mixed thoroughly in a Wig-L-Bug for five minutes under dry N_2 in a glove box. A portion of the mixed sample, ~150 mg, was weighed, degassed, and pelletized also under dry N_2. The transmission spectrum of the resulting pellet was obtained from 256 scans with a nominal resolution of 8 cm^{-1} in the 4000–600 cm^{-1} region. A reference spectrum of KBr was subtracted to yield the final clay spectrum. The system software was capable of baseline correction, subtraction, and peak deconvolution of the spectra measured.

Preparation and characterization of pillared clays

The procedure followed for the preparation of a hydroxy-Al_{13} oligocationic solution was similar to that given by Lahav *et al.* (1978). It involved gradual mixing of 23.1 cm^3 of an aqueous NaOH solution and 12.5 cm^3 of an aqueous $AlCl_3$ solution (both at a concentration of 0.2 mole dm^{-3}), and maintaining the ratio of OH^-/Al^{3+} at 2.0. The pH of the resultant solution was 4.2. This solution was aged by refluxing for 6 hours at 90°C (Tokarz and Shabtai, 1985). The aging caused a drop in pH to 3.85.

The procedure used in the preparation of pillared clays was the same as previously described (Tokarz and Shabtai, 1985). A specific feature of this procedure is that the smectite dispersion and the pillaring reagent solution are reacted in accurately predetermined constant ratios, and the product is quickly and continuously removed from the reaction zone. In all preparations, the product mixture was allowed to stand for 15 hr before the supernatant was siphoned off. The pillared clay was washed with deionized water until chloride-free, centrifuged, and freeze-dried.

All pillared clays were characterized by measuring their XRD profiles. The X-ray diffraction patterns were obtained with a Philips Norelco diffractometer, using CuKα radiation and a graphite monochromator. The thermal stabilities of the pillared clay products were determined by subjecting them to heat treatment at several selected temperatures between 300–600°C, using a Sybron Thermoline furnace. These experiments were carried out using 100 mg samples of each of the pillared clays. The samples were placed in 5 ml porcelain crucibles and inserted in a small sandbath to attain uniform temperature. The samples were heated in ambient air and the temperature of the sandbath measured by a K-type thermocouple. A new set of samples was used for each reaction temperature. The samples were allowed to remain in the furnace for 4 hours, after which they were cooled in a desiccator. Basal spacings of the thermally-treated smectites were determined by XRD, as described above.

RESULTS AND DISCUSSION

FTIR spectra of non-deuterated montmorillonites

As indicated in Table 1 the smectite samples from Wyoming, South Dakota, and Rokkaku (designated as S-WY, S-SD, and S-ROKK, respectively) have been classified as Wyoming-type montmorillonites, whereas those from Arizona, California, and Itoigawa (designated as S-AZ, S-CA, and S-ITOI, respectively) have been classified as Cheto-type montmorillonites (Grim and Kulbicki, 1961).

The FTIR absorption profiles of all the montmorillonite samples show general similarity in the 1500–4000 cm^{-1} region, as seen in Figure 3. The main absorption bands in montmorillonites, as previously assigned (Farmer, 1979; Van der Marel and Beutelspacher, 1976), are summarized in Table 3. The band near 3630 cm^{-1} has been assigned to the stretching vibration of structural OH groups attached to either Al^{3+} or Mg^{2+}. This is in agreement with the model of Hofmann *et al.* (1933), which assumes the presence of octahedral OH groups only. In the 700–1500 cm^{-1} region, the similarities among the smectites are less pronounced. The absorption bands in this region have been assigned to stretching vibrations of Si–O and Si–O–Si bonds, and also to deformation modes of OH groups attached

https://doi.org/10.1346/CCMN.1992.0400110 Published online by Cambridge University Press

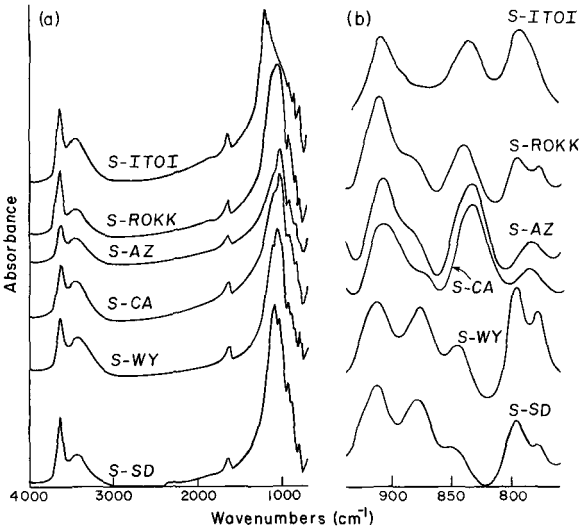

Figure 3. FTIR spectra of non-deuterated smectites in the Na-form: (a) 700–4000 cm^{-1} range; (b) detail of 700–950 cm^{-1} range.

to various ions, e.g., Al^{3+}, Mg^{2+} and Fe^{3+}. Two bands observed at 918 cm^{-1} and 888 cm^{-1} have been specifically assigned to OH groups attached to Al^{3+} and Fe^{3+} ions, respectively (Table 3).

FTIR spectra of deuterated smectites

The absorbance region of primary interest in the FTIR spectra of the deuterated smectite samples lies between 2600–2750 cm^{-1}. This is the expected range for the O–D stretching band. An example of the FTIR spectrum of the deuterated S-AZ smectite sample is shown in Figure 4. There are two bands (at 2675 and 2703 cm^{-1}) appearing in the O–D stretching region, indicating the presence of two different types of structural OH groups in the starting smectite. The extent of deuteration under the conditions we employed is rather low, as indicated by the major intensity difference in the absorbancies of the O–H (near 3640 cm^{-1}) and O–D bands. This is probably due to D → H exchange in the O–D groups by interaction with trace amounts of residual interlayer water, or by possible minor contact with outside moisture during the procedure, in spite of the carefully controlled conditions. It should be noted that a high extent of deuteration would require treatment of the clay with D_2O vapor under strictly controlled conditions. However, partial deuteration by the reflux method has also been observed by other authors (Fripiat, personal communication, 1990). Further, the

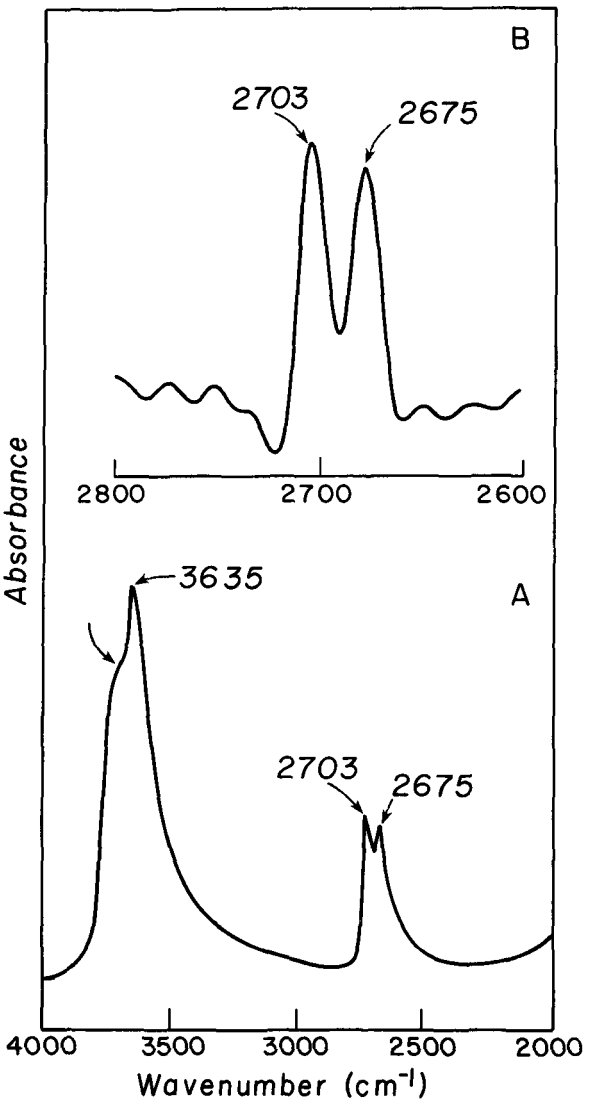

Figure 4. Resolution of two O–D stretching bands (at 2675 and 2703 cm^{-1}) in the FTIR spectrum of S-AZ: (A) non-deconvoluted; (B) deconvoluted bands. (Adsorbed water bands near 3430 cm^{-1} subtracted.)

Table 3. Tentative assignments of absorption maxima in IR spectra of montmorillonites.

Band position wave number, cm^{-1}	Assignment[1,2]
3634	O–H stretching, (Mg, Al)–OH
3433	H–O–H hydrogen bonded water
1635	H–O–H deformation
1115	Si–O stretching in-plane
1040	Si–O–Si stretching
918	Deformation of OH linked to $2Al^{3+}$
888	Deformation of OH linked to Fe^{3+} and Al^{3+}
847	Deformation of OH linked to Al^{3+} and Mg^{2+}
778	Si–O deformation perpendicular to optical axis
671	Si–O deformation parallel to the optical axis

[1] Van der Marel, H. W. and Beutelspacher, H. (1976).
[2] Farmer, V. C. (1979).

https://doi.org/10.1346/CCMN.1992.0400110 Published online by Cambridge University Press

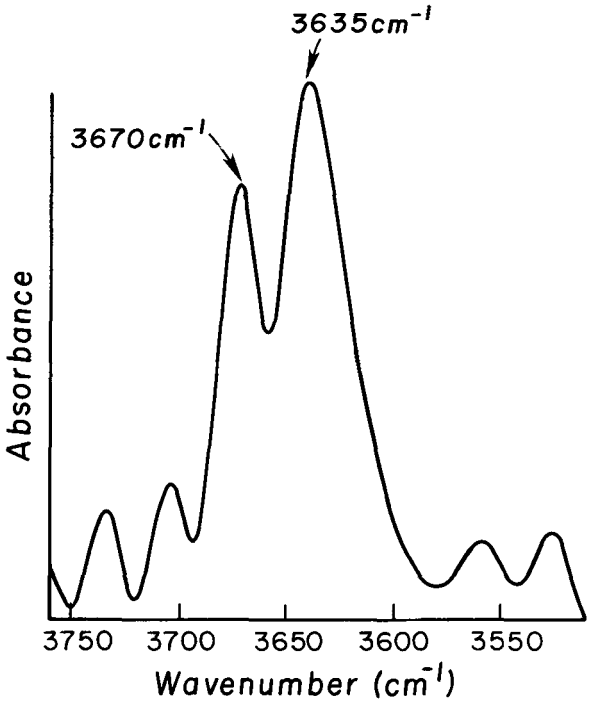

Figure 5. Resolution of two O–H stretching bands in the FTIR spectrum of non-deuterated and partially dehydroxylated S-CA (deconvoluted bands).

low extent of deuteration observed in the present study was advantageous for resolving the two different O–D bands. Indeed, some difficulty in resolving the two corresponding O–H bands in the non-deuterated smectites was probably due to overlap of the two anticipated bands. However, resolution of these two bands was achieved after short calcination (30 min at 600°C). This caused partial dehydroxylation and an attendant decrease in the intensity of the two bands. An example of the separation of an OH band near 3635 cm^{-1} and another OH band near 3670 cm^{-1} is given in Figure 5. For differentiation of the two O–D bands in the following text, they are designated as $(O–D)_h$ for the higher frequency and $(O–D)_l$ for the lower frequency band. As shown below, for homoionic Wyoming-type montmorillonites the position of the higher frequency band is in the range of 2714–2728 cm^{-1}, whereas for Cheto-type montmorillonites it is between 2702–2706 cm^{-1}. The lower frequency band is in the narrow range of 2674–2684 cm^{-1} for both montmorillonite types.

Figure 6 shows the change in relative intensity of the two O–D stretching bands as a function of the nature of the smectite (in the homoionic Li form). For the two deuterated Wyoming-type montmorillonites, viz., the S-SD and S-WY samples, the $(O–D)_l$ band is markedly stronger than the $(O–D)_h$ band (as measured by peak areas). For the three Cheto-type montmorillonites (Table 1), as well as for the S-ROKK sample, however, the relative intensity of the $(O–D)_h$ band is dramatically

Table 4. Comparison of the MgO/Al_2O_3 weight ratios in smectites with the $(O–D)_h/(O–D)_l$ band intensity ratios.

Smectite (type)	MgO/Al_2O_3 weight ratio	$(O–D)_h/(O–D)_l$ band intensity ratio	
		Li-form	Ca-form
S-SD (Wyoming)	0.135	0.27	0.28
S-WY (Wyoming)	0.147	0.42	0.23
S-ITOI (Cheto)	0.336	1.02	0.79
S-AZ (Cheto)	0.377	0.78	0.88
S-CA (Cheto)	0.488	0.70	0.61

increased; for the S-ITOI and S-ROKK samples it actually becomes stronger than that of the $(O–D)_l$ band.

One could consider two possible explanations for the observed resolution of the O–D stretching into two bands. The simplest and most plausible interpretation is that the two bands are due to two types of octahedral OH groups, i.e., AlAlOH and AlMgOH, as anticipated from Hofmann's model of montmorillonite (Figure 1). Such an assignment would require some degree of relationship between the Mg/Al ratios in the smectites and the observed $(O–D)_h/(O–D)_l$ intensity ratios. As shown in Table 4, there is good qualitative correspondence between the above two ratios. The two Wyoming-type smectites (S-SD and S-WY), which are characterized by low MgO/Al_2O_3 ratios, show low $(O–D)_h/(O–D)_l$ intensity ratios, whereas the Cheto-type smectites (S-AZ, S-CA and S-ITOI), which have markedly higher MgO/Al_2O_3 ratios, exhibit significantly higher $(O–D)_h/(O–D)_l$ ratios. Thus, it is plausible that the $(O–D)_h$ band is due to AlMgOD groups, whereas the $(O–D)_l$ band originates from AlAlOD groups. The tentative assignment of the higher O–D frequency band between 2702–2728 cm^{-1} to AlMgOD is in agreement with a previous tentative detection of such a band between 2700–2705 cm^{-1} by Russell and Fraser (1971).

Another, less plausible possibility is that the $(O–D)_h$ band between 2702–2728 cm^{-1} is due to deuterated tetrahedral OH, e.g., silanol (Si–OH) groups at the internal surface (Figure 2). Some literature data on silanol groups in materials other than smectites, e.g., Cab-O-Sil silica (Cabot Corp., 1987) or H-ZSM-5 zeolite (Qin *et al.*, 1985), indicate the presence of higher-frequency bands (between 3720–3745 cm^{-1}) than the band frequency reported by Farmer (1979) for octahedral AlAlOH and AlMgOH groups (3634 cm^{-1}; see Table 3). Beidellite, which is generally assumed to contain surface Si–OH groups, has been reported (Schutz *et al.*, 1987) to absorb near 3440 cm^{-1}. The assignment of this band to tetrahedral Si–OH groups, however, may be in doubt, since its frequency is apparently outside the usual nonassociated O–H stretching region (3500–3700 cm^{-1}) for both inorganic and organic compounds. Indeed, it is not excluded that the band near 3440 cm^{-1} observed by Schutz *et al.* (1987) was due to adsorbed water, which should show a strong band near 3430 cm^{-1}.

https://doi.org/10.1346/CCMN.1992.0400110 Published online by Cambridge University Press

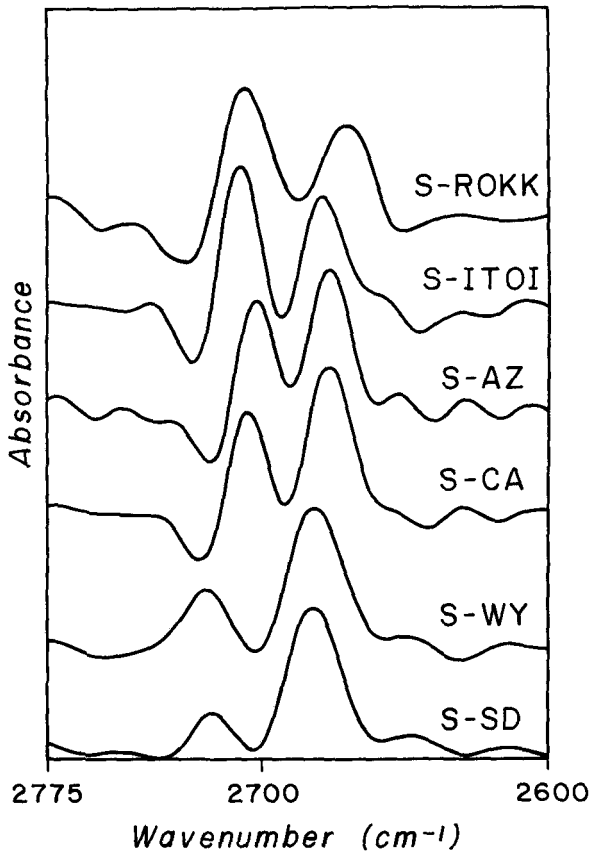

Figure 6. Relative intensities of the $(O–D)_h$ and $(O–D)_f$ stretching bands as a function of smectite type (Li-exchanged smectites).

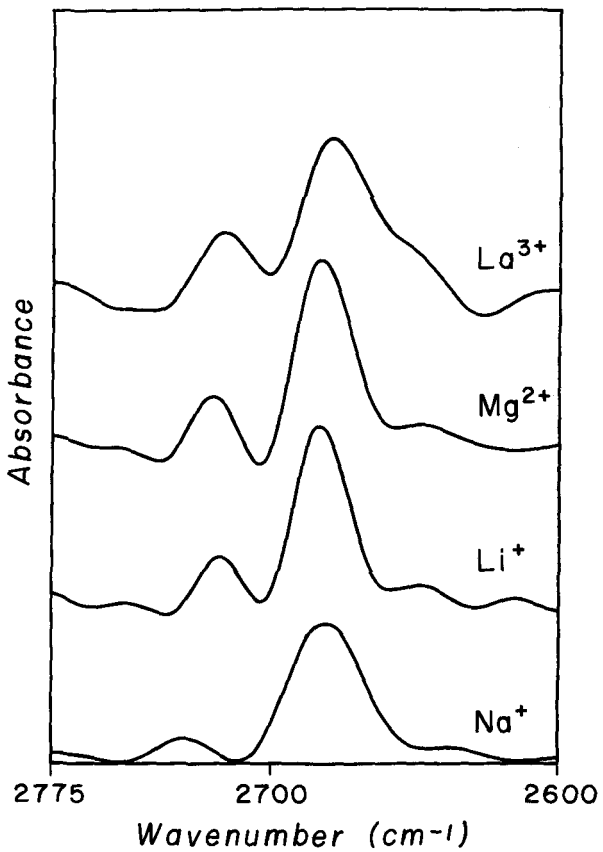

Figure 7. Effect of exchangeable cation upon the relative intensities of the $(O–D)_h$ and $(O–D)_f$ bands (S-SD; Wyoming type).

Effect of interlamellar cations upon the relative intensities of the two O–D stretching bands

The effect of the exchangeable cation, i.e., Li^+, Na^+, Mg^{2+}, Ca^{2+}, or La^{3+}, upon the relative intensities of the $(O–D)_h$ and $(O–D)_f$ bands of partially-deuterated Wyoming- and Cheto-type montmorillonites was also investigated. Figure 7 summarizes the results obtained for the S-SD Wyoming-type sample. The relative intensity of the $(O–D)_h$ band for this smectite was considerably weaker than that of the $(O–D)_f$ band, but it increased slightly with increase in the Lewis acidity (electron density) of the exchangeable cation in the order $La^{3+} > Mg^{2+} > Li^+ > Na^+$. A similar, but somewhat stronger, effect was found for the other Wyoming-type montmorillonite (S-WY) examined, as shown in Figure 8. The two Cheto-type montmorillonites, S-AZ and S-ITOI, showed a different pattern, as indicated in Figures 9 and 10, respectively. The $(O–D)_h$ band was of approximately equal (Figure 9) or slightly higher (Figure 10) intensity relative to that of the $(O–D)_f$ band. Furthermore, the relative intensity of the $(O–D)_h$ band changed only slightly with increase in cation acidity. Closely similar behavior was observed for the S-CA smectite belonging to the Cheto-type clays. The S-ROKK sample, which has been tentatively classified as a Wyoming-type montmorillonite (Grim and Kulbicki, 1961), shows greater similarity to the Cheto-type smectites in the O–D stretching range.

The observed slight-to-moderate increase in the relative intensity of the $(O–D)_h$ band for Wyoming-type montmorillonites with increase in cation charge density (Figures 7, 8) may be indicative of a certain interaction between the $(O–H)_h$, e.g., AlMgOH, groups and the interlamellar cation. For the Cheto-type montmorillonites, which showed a sharply higher $(O–D)_h$ stretching band intensity (Figures 9, 10) the effect of the interlamellar cation is somewhat more difficult to discern.

Thermal stabilities of pillared Wyoming- and Cheto-type montmorillonites

The thermal stabilities of products obtained by pillaring of the Na-forms of all smectites listed in Table 1 (except for the borderline case of S-ROKK) were investigated by measuring their basal spacings after heating for 4 hr at four different temperatures between

https://doi.org/10.1346/CCMN.1992.0400110 Published online by Cambridge University Press

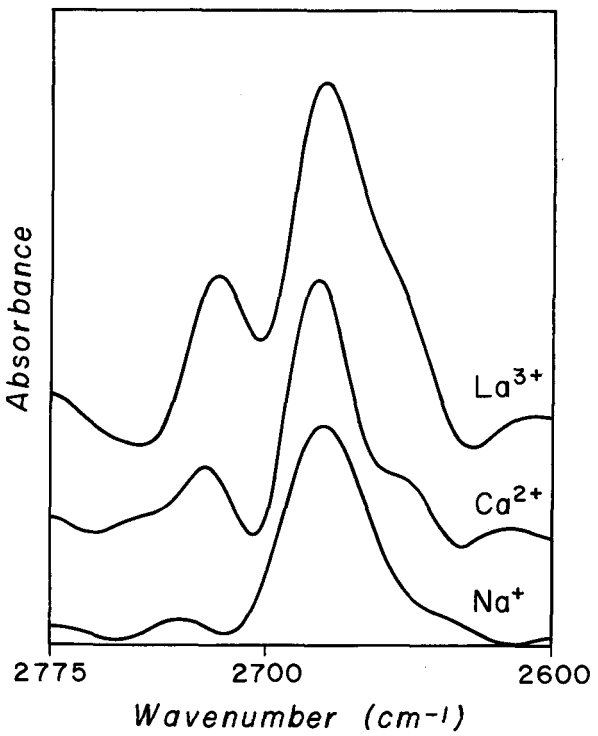

Figure 8. Effect of exchangeable cation upon the relative intensities of the $(O–D)_h$ and $(O–D)_l$ bands (S-WY; Wyoming type).

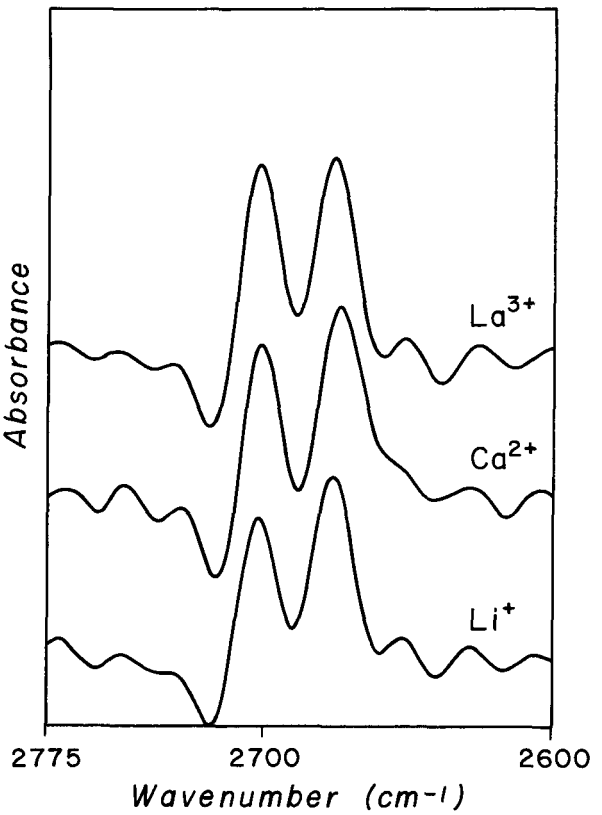

Figure 9. Effect of exchangeable cation upon the relative intensities of the $(O–D)_h$ and $(O–D)_l$ bands (S-AZ; Cheto type).

300–600°C. Results obtained are summarized in Table 5. Before heat treatment, all freeze-dried, pillared products showed basal spacings in the narrow range of 18.4–18.8 Å, in agreement with previous findings (Tokarz and Shabtai, 1985). For the pillared Cheto-type montmorillonites, heating at increasing temperatures from 300° to 600°C resulted in a relatively small decrease in d(001) values from ~18.5 Å at 25° to ~17.0 Å at 600°C. The stability of these pillared products is particularly pronounced between 400–500°C where the d(001) values remain essentially constant at 17.7 Å. For the Wyoming-type montmorillonites, on the other hand, the decrease in d(001) values is considerably steeper, i.e., from ~18.5 Å at 25° to ~15.5 Å at 600°C. This decrease is particularly steep between 400–500°C, a range in which there is no change in d(001) values for the pillared Cheto-type montmorillonites. This difference in behavior is exemplified for the S-CA (Cheto-type) and S-WY (Wyoming-type) montmorillonites in Figure 11.

Dependence of pillared smectite stability upon structural and other factors: Pillaring mechanism

It can be expected that in the initial, ion-exchange stage of the pillaring process, the hydroxy-Al_{13} oligocations are held in the interlamellar space solely by electrostatic attraction. Upon calcination at high temperatures, e.g., 400–650°C, of properly-prepared pillared clay samples [Tokarz and Shabtai (1985), Sterte and Shabtai (1987)], a gradual process of dehydrative interaction between the internal surface and the intercalated hydroxy-Al_{13} oligocations apparently takes place. This results in the formation of stable, covalent Si–O–Al bonds (or Si–O–Si bonds in the case of hydroxy–SiAl oligocations), as previously proposed by Pinnavaia *et al.* (1985), and by Sterte and Shabtai (1987). Figure 12 indicates schematically such a possible transition in the type of bonding.

Recent ^{27}Al and ^{29}Si NMR studies of pillared clays by Plee *et al.* (1985, 1987) have indicated that pillaring

Table 5. Basal spacings of pillared products from Wyoming- and Cheto-type montmorillonites as a function of calcination temperature.

Temperature (°C)	Wyoming		Cheto		
	S-WY	S-SD	S-AZ	S-CA	S-ITOI
25[1]	18.6	18.4	18.4	18.6	18.8
300	16.8	17.0	18.0	18.2	17.7
400	16.9	17.0	17.7	17.7	17.7
500	16.1	16.1	17.7	17.7	17.7
600	15.4	15.6	16.8	17.0	17.0

[1] Freeze-dried, pillared smectite (no heat treatment applied).

https://doi.org/10.1346/CCMN.1992.0400110 Published online by Cambridge University Press

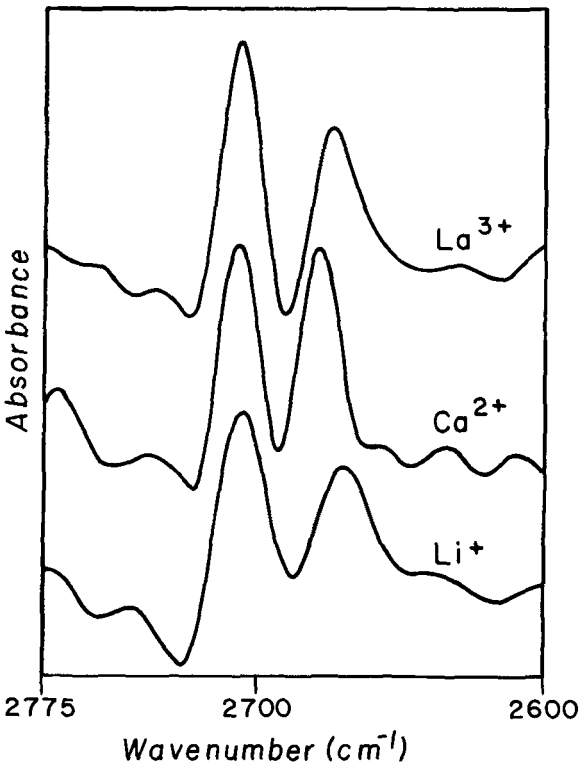

Figure 10. Effect of exchangeable cation upon the relative intensities of the $(O–D)_h$ and $(O–D)_f$ bands (S-ITOI; Cheto type).

with hydroxy-Al_{13} of smectites lacking tetrahedral substitution, e.g., hectorite and laponite, followed by very mild calcination (400°C), caused no reaction between intercalated Al_{13} species and the smectite; no structural changes were observed in either of the two reactants. However, smectites with tetrahedral substitution, e.g., synthetic beidellite, under the same conditions were found to undergo a major cross-linking reaction with the intercalated hydroxy-Al_{13}, as evidenced by profound structural changes both in the smectite and in the pillaring oligocation. Due to the apparent low thermal stability of the pillared clay samples prepared by Plee *et al.* (1985), no evidence regarding the nature of possible pillaring reactions at higher calcination temperatures, e.g., 400–650°C, was obtained in their NMR work.

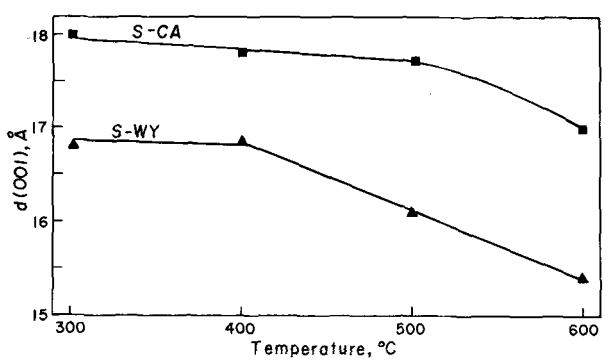

Figure 11. Change in d(001) as a function of calcination temperature for S-CA (Cheto type) and S-WY (Wyoming type).

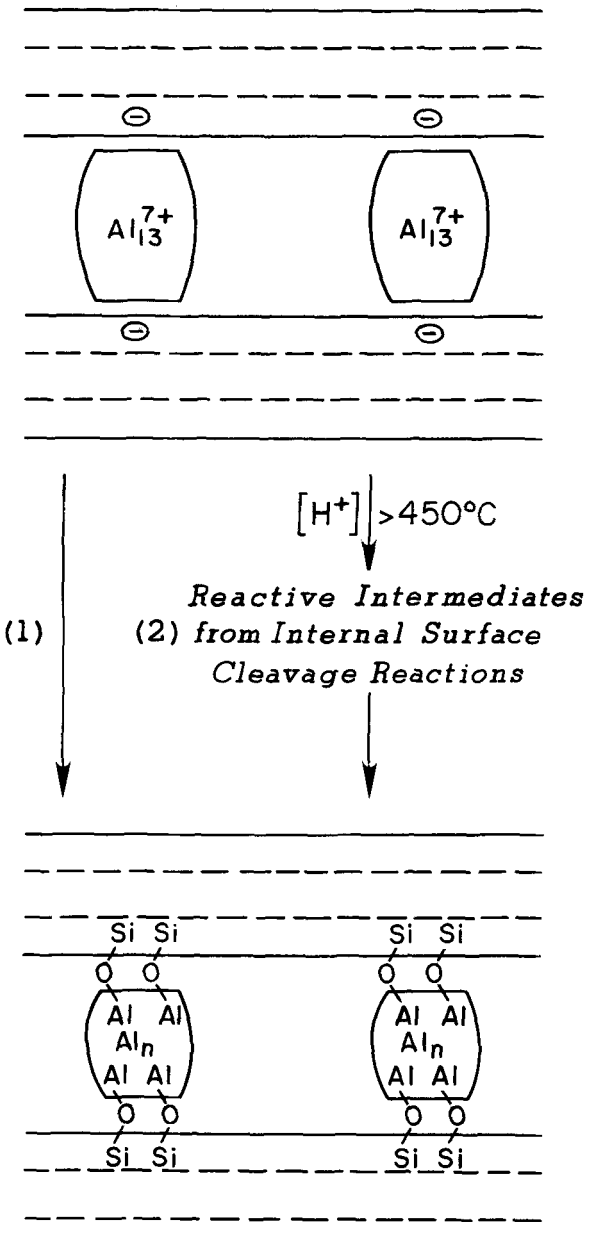

Figure 12. Schematic presentation of probable high-temperature transition from electrostatic to covalent bonding in pillared smectites ($Al_{13}^{7+} = [Al_{13}O_4(OH)_{24}(H_2O)_{12}]^{7+}$).

There are several factors that could be considered to explain the observed higher thermal stability of pillared Cheto as compared with Wyoming-type montmorillonites. One of the factors is the cation exchange capacity (or charge density) of the smectites, which in

https://doi.org/10.1346/CCMN.1992.0400110 Published online by Cambridge University Press

turn could determine the population density of the pillaring species. The higher CEC values for Cheto-type montmorillonites (Table 1) are qualitatively consistent with the higher thermal stability of their pillared products. However, the relationship does not seem to be quantitative as the pillared S-ITOI smectite (CEC = 115 meq/100 g) shows equal, or slightly better, thermal stability (Table 5) as compared with that of pillared S-AZ smectite (CEC = 137 meq/100 g). Previous work on partially-pillared smectites (Tokarz and Shabtai, 1985) has shown that such products possess high thermal stability even at a moderately high (75–80%) extent of pillaring. Therefore, it is likely that a high population density of the pillaring species is only a contributing factor to thermal stability.

Another factor to be considered is the difference in octahedral substitution pattern in the two types of montmorillonites and its effect upon the thermal stability of the smectite component in the corresponding pillared products. Specifically, the iron-rich Wyoming-type smectites could be expected (Grim, 1968) to possess lower thermal stability as compared with the low Fe-content Cheto-type montmorillonites (Table 2). It was shown in previous studies (Shabtai *et al.*, 1985) that the thermal stability of the smectite component does indeed affect the stability of the pillared product. A thermally stable and dehydroxylation-resistant fluorhectorite yielded a considerably more stable hydroxy-Al_{13} pillared product as compared with that derived from a less stable, nonfluorinated hectorite.

Finally, a possible difference in the extent of covalent bonding between the internal surface and the hydroxy-Al_{13} oligocations for the two types of smectites could be considered. High temperature (>450°C) treatment of pillared smectites has been shown to result in a stable, zeolite-like molecular sieve system with well-defined pore-size distribution (Tokarz and Shabtai, 1985). In view of other studies (Pinnavaia *et al.*, 1985; Plee *et al.*, 1987; Sterte and Shabtai, 1987) it can be assumed that covalent bonding involves dehydrative-dehydroxylating interaction of the hydroxy-Al_{13} (or hydroxy-SiAl) oligocations with either preexistent tetrahedral OH groups (Figure 2), especially in the case of beidellite, or with OH (or other reactive groups) formed as intermediates by high-temperature cleavage reactions of the internal layer surface (Figure 12, pathways (1) and (2), respectively). Such reactions may be strongly catalyzed above 450°C by intercalated acidic oligocations, and may be essential for stable montmorillonite pillaring. The indicated higher concentration of AlMgOH groups in Cheto-type montmorillonites may have the effect of increasing the reactivity of the internal surface (or some sites on this surface, e.g., inverted tetrahedra) for such cleavage reactions and the extent of attendant or subsequent covalent bonding with the pillaring species. Clarification of the chemistry of high temperature (>450°C) crosslinking reactions in smectites would obviously necessitate further NMR studies.

It should be noted that the vast majority of previous studies on pillared clays have been performed with Wyoming-type montmorillonites as feeds, resulting in products of low thermal stability, and, consequently, limited applicability as catalysts. Natural beidellites do not offer a realistic alternative in view of their scarcity. Therefore, the present results indicate that Cheto-type montmorillonites should be considered as starting materials of choice in future studies, leading eventually to thermally stable catalyst systems.

SUMMARY AND CONCLUSIONS

A systematic FTIR study of partially-deuterated Cheto- and Wyoming-type montmorillonites (MS) revealed the presence of two O–D stretching bands, one between 2702–2728 cm^{-1} and another near 2680 cm^{-1}, designated as $(O–D)_h$ and $(O–D)_l$, respectively. The observed spectral resolution was attributed to the presence of two types of octahedral O–H groups in the original smectites. Based on the relationship between the MgO/Al_2O_3 weight ratios in the smectites, and the $(O–D)_h/(O–D)_l$ intensity ratios, the $(O–D)_h$ band was assigned to AlMgOH and the $(O–D)_l$ to AlAlOH groups. For Wyoming-type MS the $(O–D)_h/(O–D)_l$ intensity ratio is low (e.g., 0.23–0.28 for the Ca-exchanged MS-forms), whereas for Cheto-type MS it is, comparatively, three to four times higher (e.g., 0.61–0.88 for the Ca-forms). This provides a convenient method for identification and differentiation of the two types of montmorillonite.

Pillaring of Cheto-type MS with hydroxy-Al_{13} oligocations resulted in products showing much higher thermal stability between 400–600°C when compared to that of identically-pillared Wyoming-type MS. This major difference in stability can be tentatively ascribed to various contributing factors, e.g., differences in CEC values (population density of the pillaring oligocations), compositional-structural characteristics, and the relative extent of covalent bonding between the internal clay surface and the pillaring species.

The present results indicate that Cheto-type MS should be considered as starting materials of choice for the preparation of thermally-stable pillared products and catalyst systems.

ACKNOWLEDGMENT

We thank Dr. K. H. Michaelian for helpful discussions.

REFERENCES

Cabot Corporation (1987) Cab-O-Sil Fumed Silica: Properties and Functions: *Cab-O-Sil Division Bull.*, p. 8–9.

Deuel, H., Huber, G., and Iberg, R. (1950) Organische Derivate von Tonmineralien: *Helv. Chim. Acta* **33,** 1229–1232.

Edelman, C. H. and Favejee, J. Ch. L. (1940) On the crystal structure of montmorillonite and halloysite: *Z. Kristallogr.* **102,** 417–431.

Farmer, V. C. (1979) *Data Handbook for Clay Materials and Other Non-metallic Minerals:* H. Van Olphen and J. J. Fripiat, eds., Pergamon Press, 285–337.

Faucher, J. A. and Thomas, H. C. (1955) Exchange between heavy water and clay minerals: *J. Phys. Chem.* **59,** 189–191.

Fripiat, J. J. (1988) High resolution solid state NMR study of pillared clays: *Catalysis Today* **2,** 281–295.

Goodman, B. A. and Stucki, J. W. (1984) The use of nuclear magnetic resonance for the determination of tetrahedral aluminum in montmorillonite: *Clay Miner.* **19,** 663–667.

Grim, R. E. (1968) *Clay Mineralogy:* 2nd ed. McGraw-Hill, New York, p. 315.

Grim, R. E. and Kulbicki, G. (1961) Montmorillonite: High temperature reactions and classification: *Amer. Mineral.* **46,** 1329–1369.

Gruner, J. W. (1934) The crystal structure of talc and pyrophyllite: *Z. Kristallogr.* **88,** 412–419.

Güven, N. (1974) Electron-optical investigations on montmorillonites. 1. Cheto, Camp Berteaux and Wyoming Montmorillonites: *Clays & Clay Minerals* **22,** 155–165.

Hayashi, H. (1963) Montmorillonites from some bentonite deposits in Yamagata Prefecture, Japan: *Clay Sci.* **1(6),** 176–182.

Hofmann, U., Endell, K., and Wilm, D. (1933) Kristallstruktur und Quellung von Montmorillonit: *Z. Kristallogr.* **86,** 340–348.

Jonas, E. C. (1955) The reversible dehydroxylation of clay minerals: *Proc. Third Natl. Clay Confer., U.S. Natl. Acad. Sci., Publ. 395,* 66–72.

Komarneni, S., Fyfe, C. A., Kennedy, G. J., and Strobl, H. (1986) Characterization of synthetic and naturally occurring clays by ^{27}Al and ^{29}Si magic angle spinning NMR spectroscopy: *J. Amer. Ceram. Soc.* **69(3),** c45–c47.

Lahav, N., Shani, U., and Shabtai, J. (1978) Cross-linked smectites. I. Synthesis and properties of hydroxy-aluminum montmorillonite: *Clays & Clay Minerals* **26,** 107–115.

Landgraf, K. F. (1979a) Distinction between Cheto and Wyoming type of montmorillonites by the effect of organic interlayers on the optical refraction: *Chem. Erde* **38,** 97–104.

Landgraf, K. F. (1979b) Distinction between Cheto and Wyoming type of montmorillonites by the relative X-ray intensities of the (001) series of the glycol complexes: *Chem. Erde* **38,** 233–244.

Lippmaa, E., Magi, M., Samoson, A., Engelhardt, G., and Grimmer, A. R. (1980) Structural studies of silicates by solid-state high resolution ^{29}Si NMR: *J. Amer. Chem. Soc.* **102,** 4889–4893.

Magdefrau, E. and Hofmann, U. (1937) Die Kristallstruktur des Montmorillonits: *Z. Kristallogr.* **98,** 299–323.

Matsumoto, M., Suzuki, M., Takahashi, H., and Saito, Y. (1986) Solid-state NMR studies on pillar-interlayered naturally-occurring montmorillonite: *Bull. Chem. Soc. Japan* **89(1),** 303–304.

McConnell, D. (1950) The crystal chemistry of montmorillonite: *Amer. Mineral.* **35,** 166–172.

Michaelian, K. H., Bukka, K., and Permann, D. N. S. (1987) Photoacoustic infrared spectra (250–10,000 cm^{-1}) of partially deuterated kaolinite #9: *Can. J. Chem.* **65,** 1420–1423.

Muller, D., Gessner, W., Behrens, H. J., and Scheller, G. (1981) Determination of the aluminum coordination in aluminium-oxygen compounds by solid-state high resolution ^{27}Al NMR: *Chem. Phys. Lett.* **79,** 59–62.

Pinnavaia, T. J., Landau, S. D., Tzou, M. S., Johnson, I. D., and Lipsicas, M. (1985) Layer cross-linking in pillared clays: *J. Amer. Chem. Soc.* **107,** 7222–7224.

Plee, D., Borg, F., Gatineau, L., and Fripiat, J. J. (1985) High-resolution solid-state ^{27}Al and ^{29}Si nuclear magnetic resonance study of pillared clays: *J. Amer. Chem. Soc.* **107,** 2362–2369.

Plee, D., Gatineau, L., and Fripiat, J. J. (1987) Pillaring processes of smectites with and without tetrahedral substitution: *Clays & Clay Minerals* **35(2),** 81–88.

Qin, G., Zheng, L., Xie, Y., and Wu, C. (1985) On the framework hydroxyl groups of H-ZSM-5 zeolites: *J. Catal.* **95,** 609–612.

Roy, D. M. and Roy, R. (1957) Hydrogen-deuterium exchange in clays and problems in the assignment of infrared frequencies in the hydroxyl region: *Geochim. et Cosmochim. Acta* **11,** 72–85.

Russell, J. D. and Fraser, A. R. (1971) I. R. spectroscopic evidence for interaction between hydronium ions and lattice OH groups in montmorillonite: *Clays & Clay Minerals* **19,** 55–59.

Sanz, J. and Serratosa, J. M. (1984) ^{29}Si and ^{27}Al high-resolution MAS-NMR spectra of phyllosilicates: *J. Amer. Chem. Soc.* **106,** 4790–4793.

Schomburg, J. (1976) Dilatometrical investigations of dioctahedral smectites: *Chem. Erde* **35,** 192–198.62.

Schutz, A., Stone, W. E. E., Poncelet, G., and Fripiat, J. J. (1987) Preparation and characterization of bidimensional zeolitic structure obtained from synthetic beidellite and hydroxy-aluminum solutions: *Clays & Clay Minerals* **35(4),** 251–261.

Solomon, D. H. and Hawthorne, D. G. (1983) *Chemistry of Pigments and Fillers:* John Wiley, New York, Chapter 1, 14–17.

Sterte, J. and Shabtai, J. (1987) Cross-linked smectites. V. Synthesis and properties of hydroxy-silicoaluminum montmorillonites and fluorhectorites: *Clays & Clay Minerals* **35(6),** 429–439.

Tennakoon, D. T., Jones, W., and Thomas, J. M. (1986) Structural aspects of metaloxide-pillared sheet silicates: *J. Chem. Soc. Faraday Trans.* **82,** 3081–3095.

Tokarz, M. and Shabtai, J. (1985) Cross-linked smectites. IV. Preparation and properties of hydroxyaluminum-pillared Ce- and La-montmorillonites and fluorinated NH_4^+-montmorillonites: *Clays & Clay Minerals* **33(2),** 89–98.

Van der Marel, H. W. and Beutelspacher, H. (1976) *Atlas of Infrared Spectroscopy of Clay Minerals and Their Admixtures:* Elsevier, Amsterdam.

Weiss, C. A., Altaner, S. P., and Kirkpatrick, R. J. (1987) High resolution ^{29}Si NMR spectroscopy of 2:1 layer silicates: Correlations among chemical shift, structural distortions, and chemical variations: *Amer. Mineral.* **72,** 935–942.

(Received 6 August 1991; accepted 11 October 1991; Ms. 2128)